

Forces in Magnetic Journal Bearings: Nonlinear Computation and Experimental Measurement

J. D. KNIGHT, Z. XIA AND E. B. MCCAUL

*Department of Mechanical Engineering and Materials Science
Duke University
Durham, NC 27706*

ABSTRACT

A method of calculating forces between magnets and shaft in an active magnetic journal bearing is presented. The method is based on two-dimensional finite element modelling of a region including both metals and free space for the determination of magnetic flux density. It includes nonlinear, single-valued magnetization functions for the metals in the magnets and shaft. The force is determined by the virtual work principle applied to the change of energy stored in the magnetic field as a function of shaft position within the clearance space. The extent of magnetic saturation in the metals is examined as a function of coil current and shaft position, and effects of one type of geometric error in magnet pole faces is considered. Results indicate that there is a coupling between coordinate directions for each magnet, and that the magnitude of coupling is strongly influenced by saturation and pole face geometry.

Forces are also measured in an experimental apparatus with geometry similar to an actuator for an active magnetic journal bearing. The measurement of forces in the steady current case is based on deflection of a calibrated beam held in clamped-clamped supports. Force as a function of position and coil current from a single magnet in the principal attractive direction is measured, as well as force in the direction normal to the principal axis. The measurements indicate that the ratio of normal force to principal force is approximately a linear function of the shaft eccentricity in the normal direction. Force from a pair of opposed magnets of equal strength is also measured, to simulate the effect of a strongly biased magnetic bearing. Since the resultant principal force is small, the ratio of the normal component of force to the principal component is large, exceeding 5 at large eccentricities and small currents.

Results of the measurements and calculations imply that significant coordinate coupling may be present in magnetic bearings and that control strategies for flexible rotor systems including active magnetic journal bearings should account for such coupling.

INTRODUCTION

Active magnetic journal bearings are increasingly being adopted to support rotating shafts because their feedback may be adjusted to attenuate or control shaft vibration. To apply the forces necessary for effective vibration control, however, an accurate method of characterizing the forces exerted by the bearing on the shaft must be used. In particular, for applications in which the clearances must be made small in order to maximize force versus weight or force versus current, both the actuator geometry and the control strategy must be optimized. Also, in flexible rotor systems where bearing motion is necessary in order to damp the system, it will be necessary to account for coordinate coupling in the actuator. Prediction of the forces from actuators similar to those of an active journal bearing is the purpose of the work described in this paper. Forces are calculated and measured in the case of steady coil

currents to quantify the amount of coupling between orthogonal axes aligned with the principal direction of magnetic attraction and the direction normal to this axis.

In previous papers [1,2] the authors described a method of calculating the forces exerted on a shaft by electromagnets of an actuator, and presented results of the calculations using linear theory. The results were compared with measured forces. In the present work, additional calculations are presented using nonlinear magnetization functions for the metals in the magnetic circuit, and measurements made using a second experimental apparatus are presented. The geometry of the magnetic actuator considered in both the calculations and the experiments is shown in Figure 1. Data are presented for the case where one magnet is energized, and for the case in which two magnets in an opposed pair are energized at the same current level, approximating cases with high bias flux.

NONLINEAR FORCE CALCULATION

An algorithm was developed to calculate the force exerted on a shaft by a magnet, considering the effects of a nonlinear magnetization characteristic for the rotor and magnet material. It uses the finite element method to solve the equation for vector magnetic potential in two dimensions. The force calculation part of the algorithm uses the fast solution method of Coulomb [3]. There are three primary stages in the determination of force: (a) modelling of the metal magnetization function, (b) iteration for the vector magnetic potential field consistent with nonlinear permeability, and (c) application of the force calculation algorithm.

Magnetization Function

For the calculations presented here, a magnetization function approximating that of silicon steel has been used. The magnetization function is nonlinear but is assumed to be single-valued; that is it does not exhibit hysteresis. The function is represented by tabular data [4] and is approximated by a cubic spline interpolation. At field intensities above 1200 A·t/m, the slope of the magnetization function is assumed to be the permeability of free space, μ_0 .

For numerical calculations, a useful representation of the magnetization function is that of Figure 2. The reluctivity of the material, H/B , or $1/\mu$, is plotted versus the square of the flux density. When this representation is used it is not necessary to calculate the field intensity at each location for every iteration, but only the flux distribution.

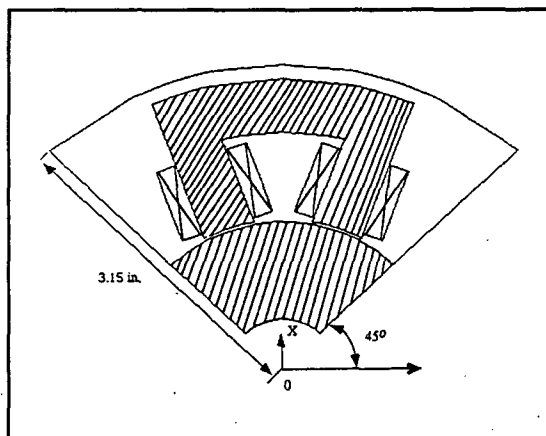


Figure 1. Calculation geometry

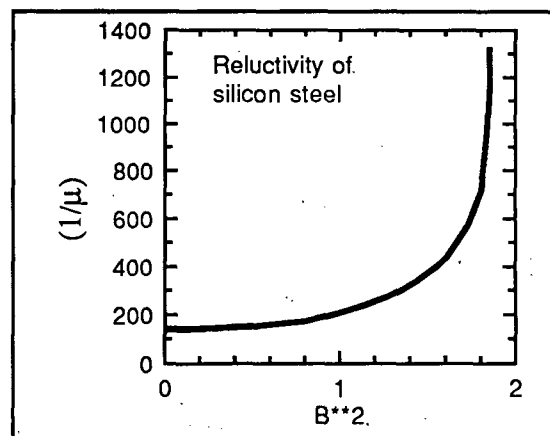


Figure 2. Reluctivity approximation

Flux Distribution

The distribution of magnetic potential, leading to the distribution of flux density, is calculated by the finite element method in two dimensions. The equation that models the potential is the nonlinear Poisson equation

$$\frac{\partial}{\partial x} \left(\frac{1}{\mu} \frac{\partial A}{\partial x} \right) + \frac{\partial}{\partial y} \left(\frac{1}{\mu} \frac{\partial A}{\partial y} \right) = -J \quad (1)$$

where μ is the magnetic permeability, J is the imposed current density and A is the magnitude of the vector magnetic potential, which in the two-dimensional case has only one component, normal to the plane of the solution region. The flux density is related to the potential by

$$\bar{B} = \nabla \times \bar{A}. \quad (2)$$

This relationship allows a convenient representation of flux density in the two dimensional case, since contours of constant A in the x,y plane are also lines parallel to \bar{B} .

The current density term J appears in those elements comprising the cross sections of the coils. It is equal to the total ampere-turns divided by the area of the coil cross-section.

An iterative method is used to obtain a potential distribution consistent with the nonlinear magnetization function. The procedure is that recommended by Silvester [5], in which a Newton-Raphson iteration is applied to determination of the reluctivity. An initial approximation to the potential is made, then updated based on successive solutions of the Poisson equation for incremental changes in the A field that result from refinement of the reluctivity distribution.

Force Calculation

When the flux distribution has been determined, the forces are calculated by the principle of virtual work. The energy change is evaluated by the method of Coulomb [3], in which only the energy changes in distorted elements are considered during a virtual displacement. It is assumed that the flux distribution is unaffected by a virtual displacement, so the force calculation requires only a single solution for the flux distribution. It is only necessary to account for the distortion of a band of elements in and near each of the air gaps.

EXPERIMENT

Apparatus

Measurements of forces exerted by electromagnets on a stationary, non-rotating shaft were made using an apparatus based on the deflection of a calibrated beam.

The magnet cores and the shaft are constructed of 0.014 inch laminations of silicon steel M15. The poles are arranged around a 3.0 inch diameter shaft with a radial clearance of 0.030 inch between magnet poles and shaft. Each magnet is wound with 400 turns of #22 wire, arranged in two coils, one on each pole leg. Each pole has a cross section of 0.375 in².

Figure 3 is a schematic of the apparatus for force measurement. The shaft is clamped at each end in a pedestal fixed to a solid base. The magnets are assembled in a retaining shell and the entire magnet assembly is mounted on a slide mechanism allowing movement in the horizontal direction. The slide is mounted in turn on a laboratory jack that allows the assembly to be moved vertically. Thus the bearing assembly can be moved in two directions and positioned accurately with respect to the fixed shaft. The relative position of the bearing is measured by four proximity probes oriented at 45° to the vertical. These probes are connected to the bearing housing so they always measure the relative displacement of the rotor from the center of the bearing regardless of the deflection of the rotor support beam.

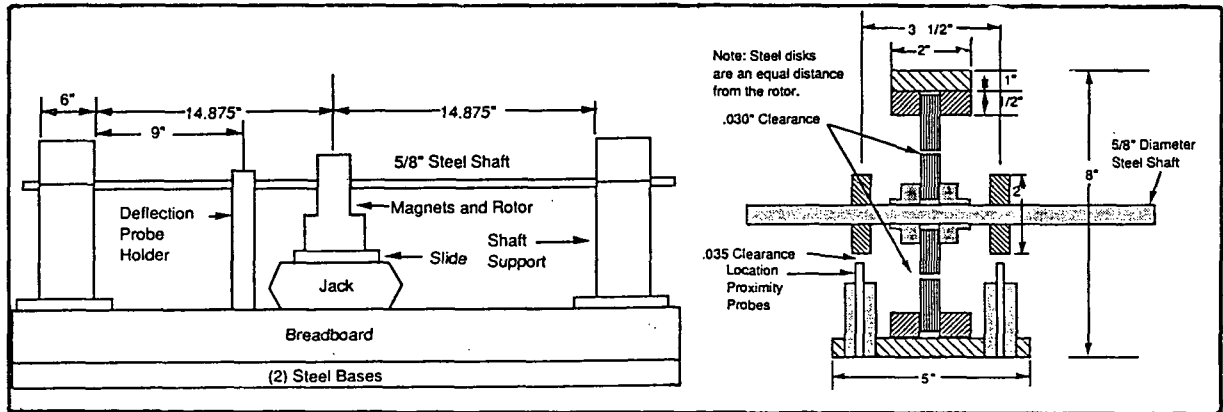


Figure 3. Force measurement schematic

When one or more of the magnets is activated, the force causes a deflection of the beam from its static position. The components of this deflection in the vertical and horizontal directions are measured by a separate set of proximity probes that are connected directly to the base of the apparatus. The force vs. deflection relationship of the structure was directly calibrated in both directions and found to be linear over the range required for measurements, so the calibrations yield a constant horizontal and a constant vertical stiffness.

Measurement Method

Before conducting force measurements, the location of the bearing center is determined by noting the position readings when the shaft is placed against the pole faces of the magnets, then interpolating to find the center.

To measure the force at a particular current level, the magnet/rotor assembly is first degaussed using alternating current in the coils of the magnet, with peak amplitude of at least twice the highest current used. The undeflected shaft position is noted. The magnets are then activated and the proximity probe outputs are read to determine the final shaft position relative to the magnets and also the absolute shaft deflection.

RESULTS OF CALCULATIONS

Calculations were performed based on the geometry of Figure 1, corresponding to the experimental apparatus and the measurements described in [2]. The forces are made dimensionless by dividing them by the force on a centered shaft predicted from 1-D magnetic circuit theory

$$F = \frac{f(2c)^2}{\mu_0 a (Ni)^2}, \quad (3)$$

where a is the pole cross sectional area, Ni is the number of amp-turns and c is the radial clearance. The magnet under consideration is an upper vertical magnet, so forces in the y -direction are the principal forces, and forces in the x -direction are the normal forces. Also plotted in the figures are the results of the linear calculation described in [2]. The effect of saturation on the force is seen in Figure 4, which shows the attractive principal force as a function of the coil current, when the shaft is in a centered position with respect to the magnet pole faces so the gap between shaft and magnet poles is constant. The force increases with current, and below 2.5 A (corresponding to 1000 A·t) the result of the nonlinear calculation is the same as that of the linear calculation. Above this value the force continues to increase, but at a much smaller rate than predicted by linear theory.

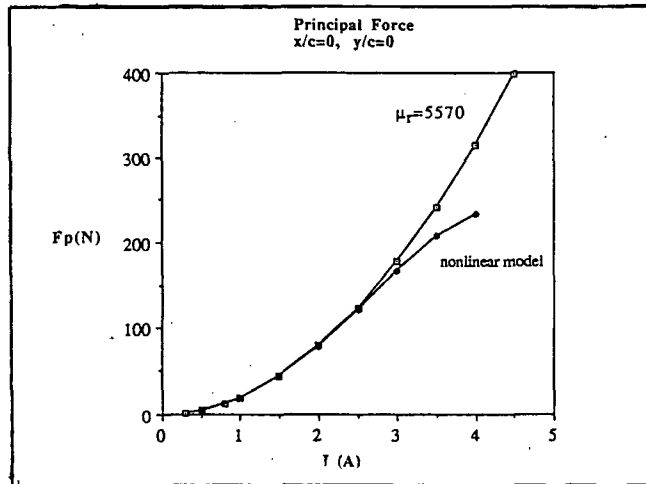


Figure 4. Calculated principal force, centered shaft

At current levels higher than 3 A the magnet material experiences saturation near the inner corners of the intersection between the pole legs and the magnet outer arc. With increasing current, the area of saturation expands across the legs. Figure 5 shows those elements that have been saturated for the case of $i = 3.5$ A. At this level of MMF the area of saturation encompasses a complete layer of elements spanning the cross-section. In this plot, saturation corresponds to a flux density of 1.4 T. At this point the slope of the magnetization function is assumed to be that of free space, so above this level of flux density the force continues to increase with current, as indicated by Figure 4, but at a much slower rate.

For a given MMF the magnet may also experience saturation when the shaft is moved closer to the magnet. Such a displacement decreases the overall reluctance of the magnetic circuit by closing the gaps, and changes the gap shape as well. Figures 6 and 7 show the increase in number of saturated elements when the shaft is moved toward the magnet, for the constant current $i = 2.0$ A. Figure 6 corresponds to a shaft eccentricity of $(X, Y) = (0, 0.5)$, which denotes a position on the magnet axis of symmetry, half the distance from the center to the maximum possible eccentricity. Elements are saturated in two areas; the inner corners of the horseshoe, and the parts of the shaft near the inner edges of the pole faces. These edges are the points of closest proximity between the poles and the rotor. As the shaft is moved closer to the magnet the areas of saturation enlarge. At an eccentricity of 0.7, Figure 7 shows the saturation areas continuing to expand. The effect on the force is illustrated in Figure 8, where the nonlinear calculation is compared with the linear solution using a relative permeability of 5570 (corresponding to silicon steel at very low field intensity). Above an eccentricity of 0.4, the force continues to increase, but at a much slower rate than predicted by linear theory.

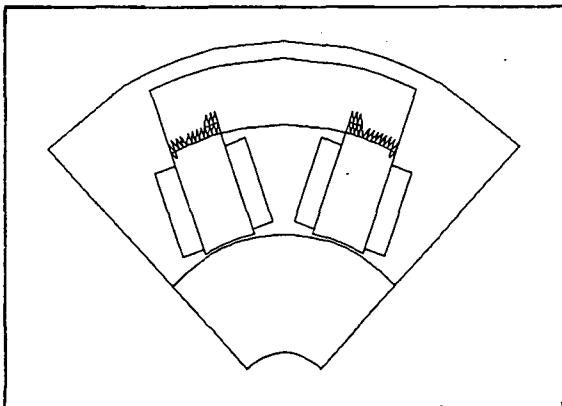


Figure 5. Saturation at 3.5 A, centered shaft

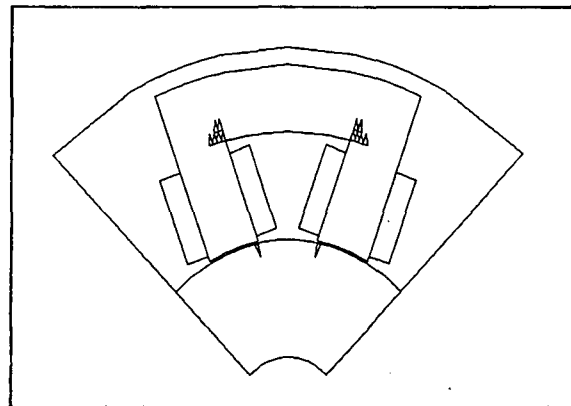


Figure 6. Saturation at 2.0 A, $y/c = 0.5$

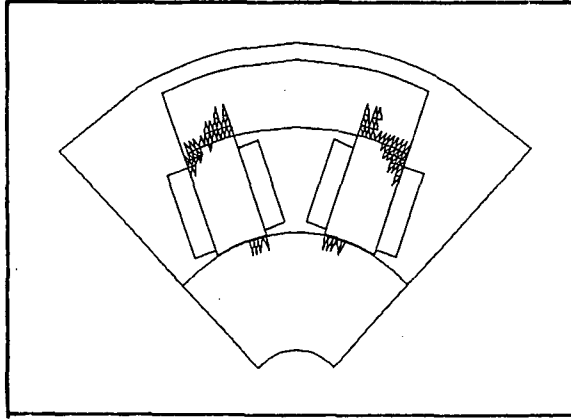
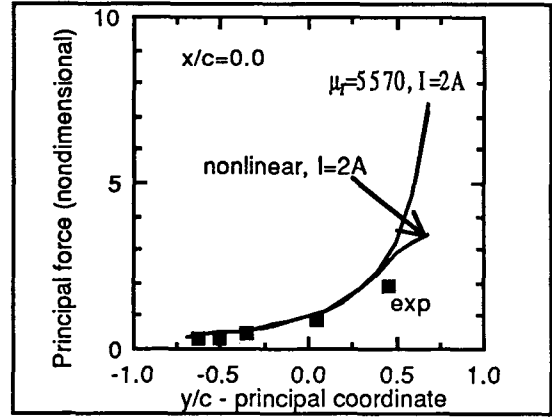
Figure 7. Saturation at 2.0 A, $y/c = 0.7$ 

Figure 8. Principal force vs. principal coord.

Asymmetry in the distribution of saturation develops when the rotor has an eccentricity off the magnet's symmetry axis. Figure 9 shows the saturation pattern when the shaft is moved to the right, to a position (0.45, 0.7), a large eccentricity. The rotor near the inner corner of the left leg is saturated, as well as almost an entire layer of elements near the right leg. The saturated region at the upper ends of the legs has also changed slightly from that of Figure 7.

The force in the normal direction is plotted in Figure 10 for one value of off-axis eccentricity, as a function of the y -position (along the symmetry axis). This force also is predicted to deviate from the linear theory above a y -displacement of 50 % of the clearance.

RESULTS OF MEASUREMENTS

Single Magnet

The apparatus described above was used to measure the force between a single magnet and the shaft for a variety of positions of the shaft with respect to the center of curvature of the magnet pole faces. Particular attention was paid to the forces when the shaft was given an eccentricity off the axis of symmetry of the magnet. Such positions, which will be seen as undesirable, may nevertheless result from three causes: misalignment of the magnets during assembly (note that this is a strong argument for manufacture of magnets having poles attached to a continuous backing ring), from dynamic motion of the shaft, or from errors in biasing.

Measurements were made at several levels of current in the magnet coils, and over a range of shaft positions within the clearance space.

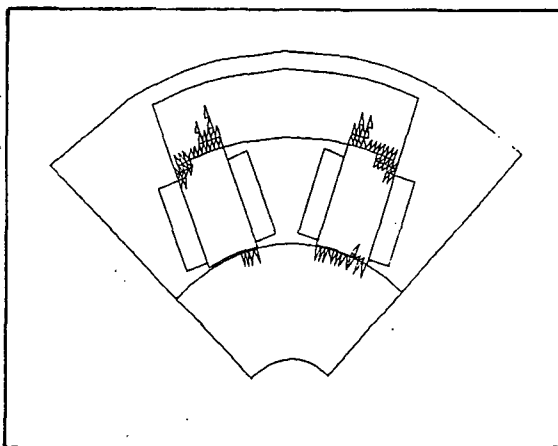


Figure 9. Saturation at large eccentricity with normal component.

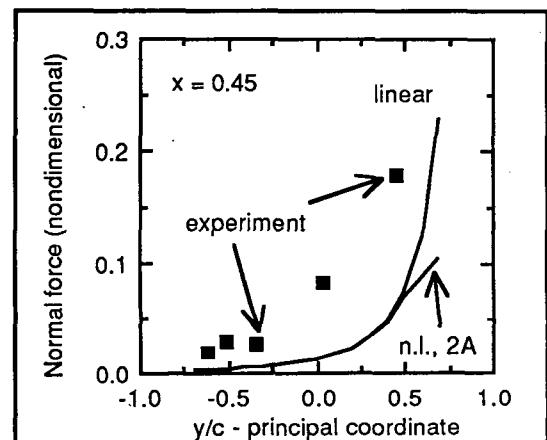


Figure 10. Normal force at 0.45 normal eccen.

In Figures 11 to 13, each group of symbols corresponds to a constant x position and therefore represents a traverse of the vertical direction (the normal direction in this case). By executing traverses of the normal direction it was possible to plot the ratio of normal force to principal force as a function of the distance away from the axis of symmetry. The value of X , or x/c , in the legend gives the position of the rotor along the axis of symmetry of the magnet. The largest possible value is 1.0. Some of the values of y/c that are presented are smaller than -1.0, corresponding to a location so far from the symmetry axis that it is outside the clearance space. While this would not be possible in an actual design, the steady state apparatus can accommodate such large displacement.

Figure 11 shows the measured force in the principal direction and Figure 12 shows the force in the normal direction at a current level of 1.0 A (400 A·t). The principal force is seen to be significantly larger at larger values of X , or rotor locations closer to the magnet. The force increases slightly as the rotor is moved away from the axis of symmetry, toward one of the poles. The magnitude of the normal force increases strongly with an increase in distance away from the symmetry axis. Figure 13 shows the ratio of the normal force to the principal force. Linear fits to the data of each traverse were calculated. To avoid confusion only one fit is shown, but the slope of this line is equal to the average of the slopes of all the fits.

Additional measurements were conducted at three other current levels, and similar trends are observed in all the cases. In each case a good linear fit to the force ratio is possible, and the slope of this fit ranges from 0.17 at 0.75 A to 0.14 at 1.5 A.

Over the ranges of position examined so far, the data indicate an approximately linear relationship between the normal eccentricity of the shaft and the ratio of normal to principal force. The constant of proportionality seems to be larger at lower currents, but for all cases examined its value is between 0.14 and 0.17. The calculations predict the existence of normal forces, but have not predicted such a large constant of proportionality for the ratio.

Opposed Magnets

The result that the normal force seems to be approximately proportional to the product of principal force and normal eccentricity indicated that the normal forces would be even more significant in the case of a strongly biased, opposed magnet pair, where the principal forces are approximately balanced. To examine this possibility a new set of experiments was conducted using two opposed magnets at the same current.

Figure 14 is a plot of the principal force exerted by the magnet pair as a function of the normal coordinate, at several values of the principal coordinate, along the symmetry axis. At small eccentricity, the force in the principal direction is near zero, as expected, since the shaft is equidistant from the two magnets. As the shaft is moved toward either of the magnets, there is

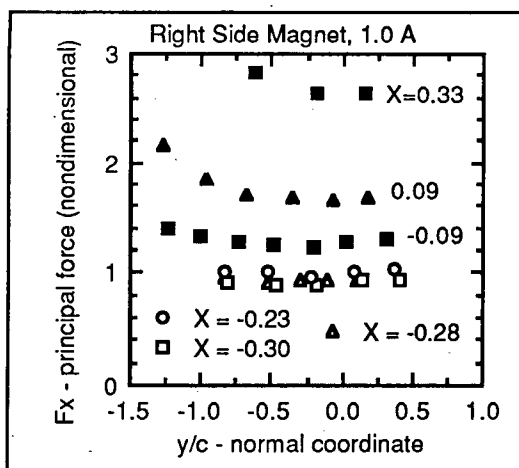


Figure 11. Principal force, single magnet

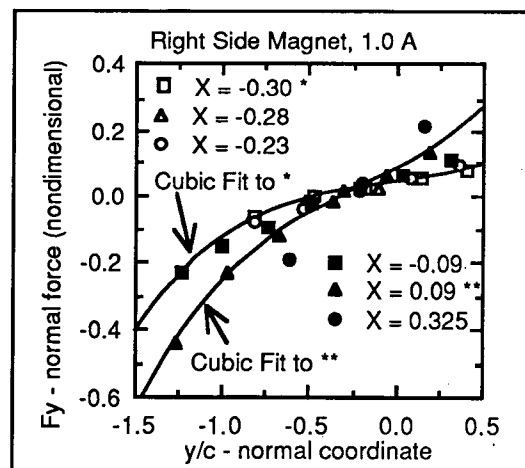


Figure 12. Normal force, single magnet

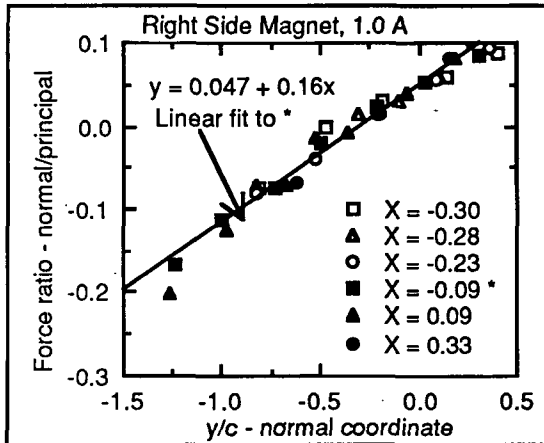


Figure 13. Force ratio, single magnet

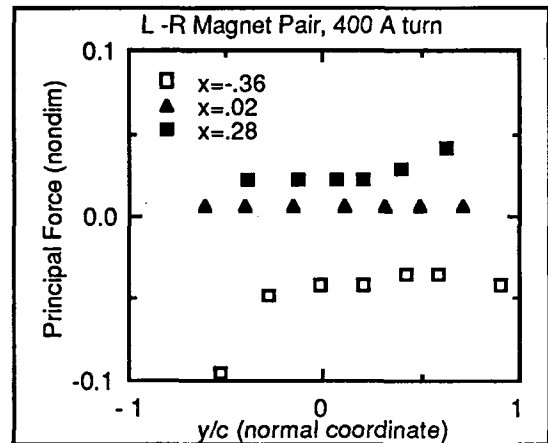


Figure 14. Principal force, opposed pair.

a resultant force in the direction of that magnet. This force is a relatively weak function of the normal coordinate, but is seen to be largest in magnitude when both normal and principal eccentricities are large.

The normal forces exerted under these conditions are shown in Figure 15. The intercept of these force plots with the axes would nominally be at (0,0), and the precise cause of their displacement from that intercept seems to be uncertainty in the angular positions of the magnets around the clearance circle. This possibility is discussed further below, but it is felt that the magnitudes of the forces observed in this plot remain significant after considering this uncertainty, because all the normal forces do in fact change sign as anticipated, at some point. The magnitude of the normal force is the same order as the resultant principal force at small eccentricities and is significantly larger than the principal force at large eccentricities, as illustrated by the plot of Figure 16, which shows the ratio of normal to principal force. This occurs because the normal forces from the two magnets are additive, while the principal forces are of opposite sign.

The displacement from zero of the intercepts of the normal forces with the axes in Figure 15 and the locations of minima of the principal forces in Figure 14 have been considered in terms of possible angular uncertainty in magnet placement. The apparatus was assembled by positioning the independent magnets against a mandrel, clamping the laminations in place, then removing the mandrel. Because of the method of assembly, it is felt that the uncertainty in radial position of each pole face is small, on the order of 1% of the clearance. The largest

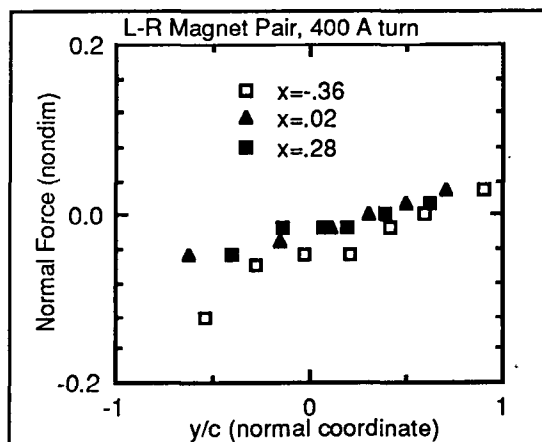


Figure 15. Normal Force, opposed pair.

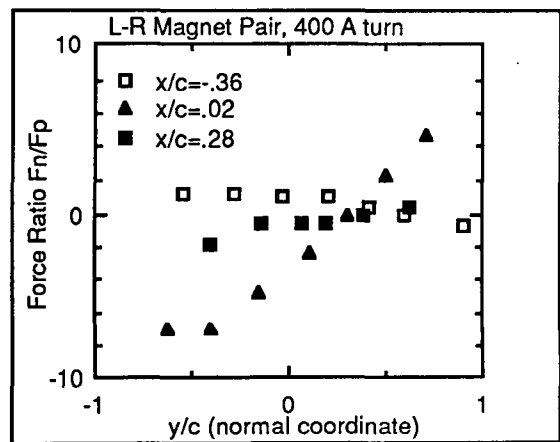


Figure 16. Force Ratio, opposed pair

uncertainty is that of the angular position of each magnet. Ideally, each magnet should be 90° from each of its neighbors, but in fact, assembly tolerances may have resulted in errors of up to 3° from the nominal positions. This would result in an uncertainty in orientation of the force vector associated with each magnet. Such a 3° uncertainty would result in an increase or decrease in the *normal* force component of approximately 2% of the *principal* force from each magnet of the pair. Using a principal force of 1.0 at zero of the principal coordinate, a 3° uncertainty in principal force orientation would result in a change in the normal force of 0.06 nondimensional force units. This is an uncertainty of the same order as the displacement of intercepts of the measured normal force data from the (0,0) position in Figure 15. If this uncertainty in angular position is the cause of the displacement of the data, it would be expected that forces measured at other current levels would behave similarly. Additional measurements were made at two other current levels, and indeed the data all are displaced by approximately the same amount. It is therefore believed that a small error in angular positioning is present.

In interpreting the measurements, then, it must be remembered that this uncertainty of angular orientation may be playing a role. Nevertheless, the magnitudes of the normal forces are still significant. Those on the negative side of the plots are apparently increased by the error, but those on the positive side are apparently decreased. Therefore, it may be conservatively stated that the magnitudes of normal forces in a magnet pair that is perfectly aligned will be at least as large as those on the positive side of the plots presented. Under this interpretation the normal forces are of significant magnitude. In addition, the very fact that the system is shown to be highly sensitive to such angular errors should receive some emphasis. This factor must be considered in designing the actuator and in determining the level of robustness or the type of algorithms required for controlling the bearing. It is a strong argument, in fact, for the use of magnets made with a continuous outer ring, which would practically preclude this type of uncertainty.

IMPLICATIONS FOR ROTOR DYNAMICS

The existence of normal forces introduces a coupling between coordinate directions that may have strong implications for the design of magnetic bearings. If the coupling is neglected, an attempt to control each magnet or each opposed magnet pair separately may result in undesirable motion.

As an example, consider a case in which the goal is to develop a linear stiffness characteristic in the principal direction by means of the active feedback. Assuming that a suitable control algorithm can be implemented, the force in the principal direction will be constrained to be a linear function of the rotor position along the axis of symmetry. The results described above indicate, however, that there will also be a normal force that is proportional to the product of the principal force and the normal eccentricity. In the case of a pair of magnets with a relatively large bias flux upon which is superposed a control flux, this implies that there will be a normal force directly proportional to distance in the normal direction; that is, a negative normal stiffness.

Consider the scenario in which all four magnets are equally and strongly biased. An arbitrary shaft displacement will be countered by changes in the principal forces from each opposed magnet pair, and the stiffnesses in these directions can be made approximately proportional to the bias flux. Each magnet pair, however, responds only to the component of displacement in its principal direction. At the same time, though, each magnet pair exerts a normal force roughly proportional to the product of its bias flux and the normal component of the displacement. The rotor will have preferred directions of oscillation along lines at 45° to the principal magnet axes. When magnets are not equally biased, the situation may be somewhat more complex.

It will be necessary to account for normal forces in designing control strategies for future generations of magnetic bearings in critical applications.

CONCLUSIONS

1. A nonlinear numerical algorithm has been developed to allow calculation of forces between a magnet and the rotor in both the principal and normal directions, allowing for arbitrary magnetization functions in the solution for magnetic flux distribution. The algorithm has been used to calculate forces based on the nominal magnetization function of silicon steel.
2. Direct measurements of forces have been made. A magnet is found to exert normal force approximately proportional to the product of the principal force and the displacement in the normal direction.
3. The measured normal forces are stronger than those that have been predicted by theory. The incorporation of nonlinear permeability with saturation into the theory, however, appears to have the effect of slightly increasing the ratio of normal to principal forces. Geometric uncertainty may further increase the force ratio.
4. The existence of significant normal force components has serious implications for the design of magnetic journal bearings, since they would result in preferred directions of oscillation of the rotor if opposed magnet pairs are independently controlled.

ACKNOWLEDGMENTS

This work was supported by NASA Lewis Research Center Grant NAG 3-968, under technical officer Dr. G. V. Brown. Additional support was received from the Lord Foundation of North Carolina.

REFERENCES

1. Knight, J. D., McCaul, E. B., and Xia, Z., "Measurement and Calculation of Forces in a Magnetic Journal Bearing Actuator," ROMAG Conference on Magnetic Bearings and Dry Gas Seals, 1991.
2. Knight, J. D., Xia, Z., McCaul, E. B. and Hacker H., "Determination of Forces in a Magnetic Journal Bearing Actuator: Numerical Computation with Comparison to Experiment," ASME Journal of Tribology, paper 91-Trib-31.
3. Coulomb, J.L, "Finite Element Implementation on Virtual Work Principle for Magnetic or Electric Force and Torque Computation", IEEE Transactions on Magnetics, Vol. MAG-20, No.5, September 1984, pp. 1894-1896.
4. Smith, R. S., Circuits, Devices and Systems, 3d ed., Wiley, New York, 1976.
5. Silvester, P., Cabayan, H.S., and Browne, B.T., "Efficient Techniques for Finite Element Analysis of Electric Machines," IEEE Trans. Power Apparatus Syst., Vol. PAS-92, No.4, pp.1274-1281, July/Aug, 1973.